International Journal of Pharmaceutics 644 (2023) 123281

Contents lists available at ScienceDirect

International Journal of Pharmaceutics

journal homepage: www.elsevier.com/locate/ijpharm

Simulation of roller compaction by combination of a compaction simulator and oscillating mill – A material sparing approach

Layla Hassan [a], René Jensen [a], Andrew Megarry [a], Lasse I. Blaabjerg [a,*]

[a] Novo Nordisk A/S, Novo Nordisk Park 2, 2760 Maaloev, Denmark
[b] F. Hoffmann-La Roche AG, Grenzacherstrasse 124, Basel, Switzerland

ARTICLE INFO

Keywords:
Compaction simulation
Roller compaction
Upscaling

ABSTRACT

This study investigates the feasibility of a compaction simulator and oscillating mill to mimic a roller compactor as a material sparing approach for process development. Microcrystalline cellulose and dicalcium phosphate dihydrate were selected to represent soft and hard materials, respectively. The relative density of ribbons and riblets was determined using a pycnometer and granules size distribution was determined by laser diffraction. Tablet tensile strength and relative density were determined using a hardness tester and pycnometer, respectively. This study showed that the relative density of riblets and ribbons were similar between 1 and 12 kN/cm, which indicates that the compaction simulator adequately mimics the compaction of the roller compactor using a Kp of 1. The size distribution of granules produced by the oscillating mill and roller compactor were similar, which indicates that the oscillating mill adequately mimics the roller compactor when using a similar gap and sieve design. Finally, the tablet tensile strength and relative density were similar independent of the applied granulation method and deformation behaviour of the material. In conclusion, the use of a compaction simulator and an oscillating mill in combination adequality mimics the roller compactor, which ultimately can save large amounts of material and time during process development.

1. Introduction

Roller Compaction is a well-established continuous granulation method. It is a particularly attractive choice when faced with components that are sensitive to heat or water, have poor blend flow properties or lead to poor tablet content uniformity. During the roller compaction process material is drawn via a feed screw between two rolls, densifying the powder into ribbons, which are then granulated with the use of a mechanical mill and chosen sieve size. The parameters including specific compaction force, roll gap width and roll speed highly influence ribbon characteristics (Zinchuk et al., 2004). An increase in specific compaction force results in ribbons with an increased relative density which in turn result in increased ribbon tensile strength (Reimer and Kleinebudde, 2019). An increase in roll gap width result in ribbons with increased thickness which in turn result in a decrease in the ribbon relative density at the same specific compaction force, which can be explained by the applied force being distributed over a larger nip area (Peter et al., 2010). An increase in roll speed may result in ribbons with decreased tensile strength, which can be explained by the reduced dwell time during compaction (Kleinebudde, 2022; Hancock et al., 2003; Souihi et al., 2015; Rowe et al., 2017). Downstream, an increased relative density of a ribbon may result in lower amount of small particles following milling, which subsequently may increase granule flowability and decrease tablet tensile strength (Bultmann, 2002). When developing a roller compaction process, ideally all the parameters mentioned above are investigated. While equipment differences such as mill, seal and feed geometry can lead to different granule properties, an early understanding of the relationship between roller compaction parameters and granule properties is critical for robust drug products design (Haeffler et al., 2019). Changes in the roller compactor scale and potentially design are common when progressing drug products from lab to clinical and finally commercial scale. As typical roller compactors used at a clinical scale consume material while reaching steady state and have an inherent dead volume, development on this equipment can be a challenge in early development where only small amounts of active pharmaceutical ingredient may be available. As a solution, material sparing process development has gained interest in recent years during the development phase of drug products (Reimer and Kleinebudde, 2019; Peter et al., 2010; Vasudevan et al., 2022). One technique which has become more common is to use a compaction simulator which can

* Corresponding author.
E-mail addresses: lasse.blaabjerg@roche.com, blaabjerg@roche.com (L.I. Blaabjerg).

https://doi.org/10.1016/j.ijpharm.2023.123281
Received 15 April 2023; Received in revised form 27 July 2023; Accepted 28 July 2023
Available online 29 July 2023

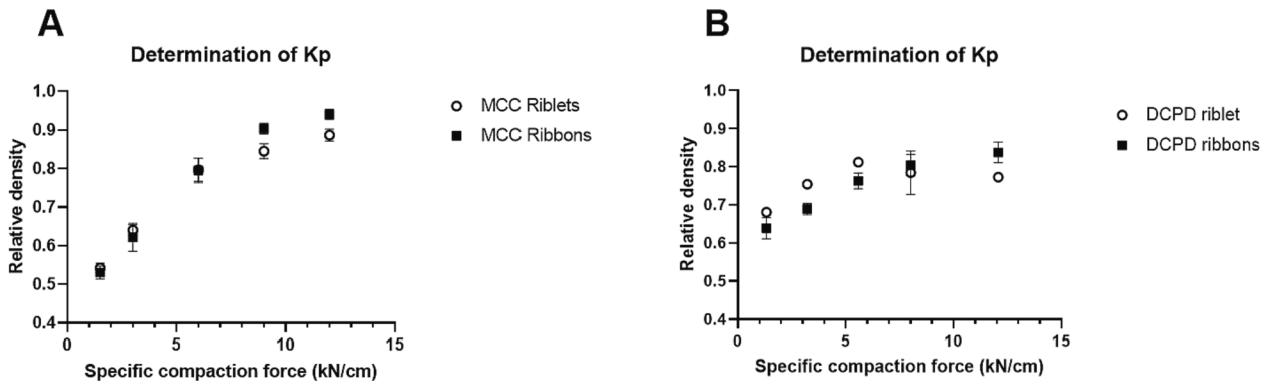

Fig. 1. Relative density of ribbons and riblets containing MCC (A) or DCPD (B) (n = 3) (mean ± SD).

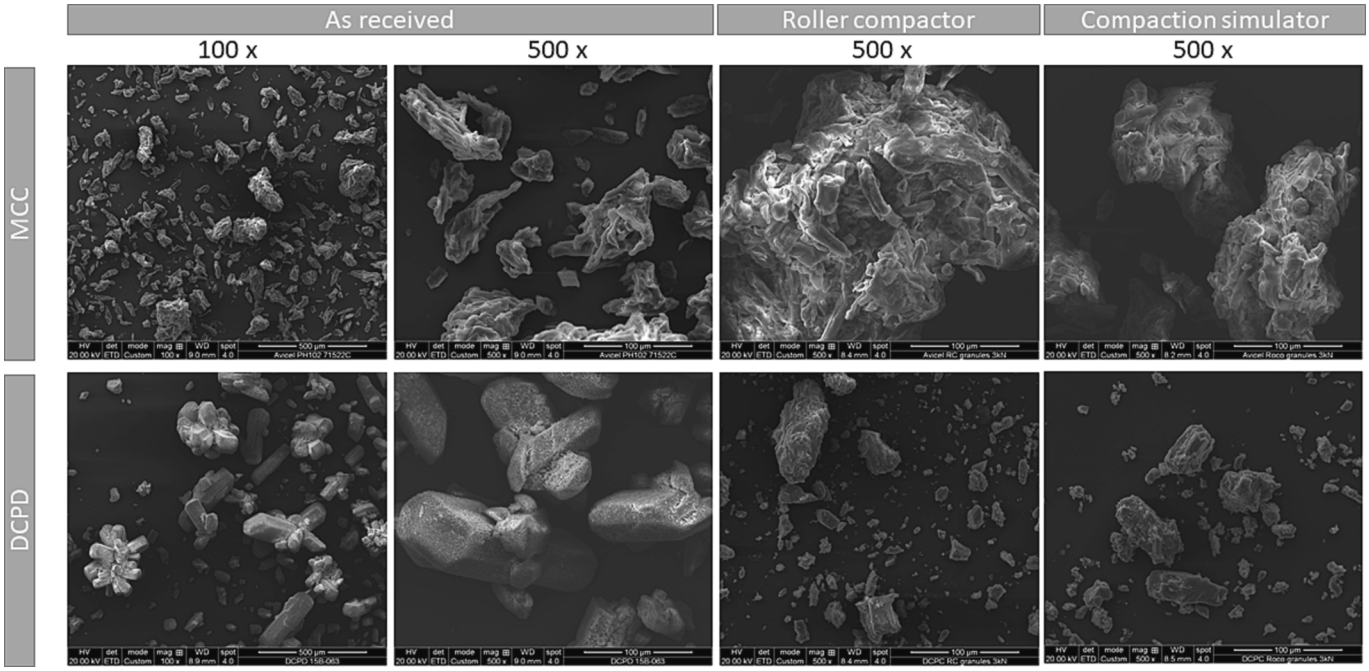

Fig. 2. Scanning electron microscopy images of MCC and DCPD as received, after roller compaction, and after roller compaction simulation followed by oscillating milling.

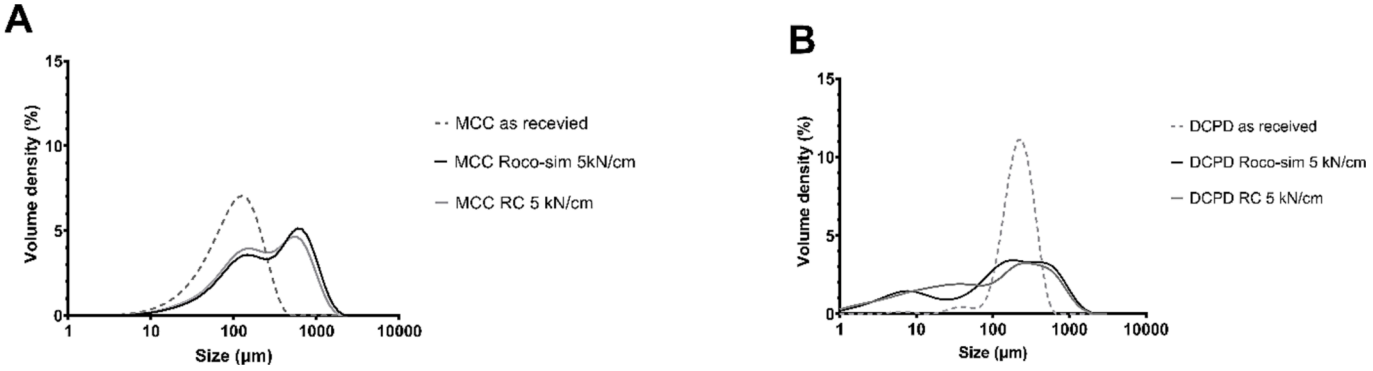

Fig. 3. PSD of MCC (A) and DCPD (B) after roller compaction simulation and roller compaction and milling.

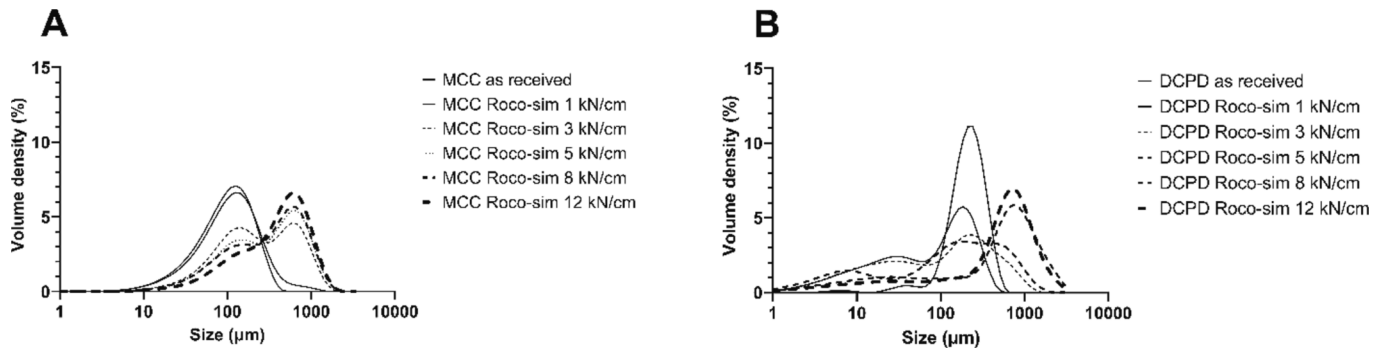

Fig. 4. PSD for MCC (A) and DCPD (B) prepared by roller compaction simulation using different specific compaction forces.

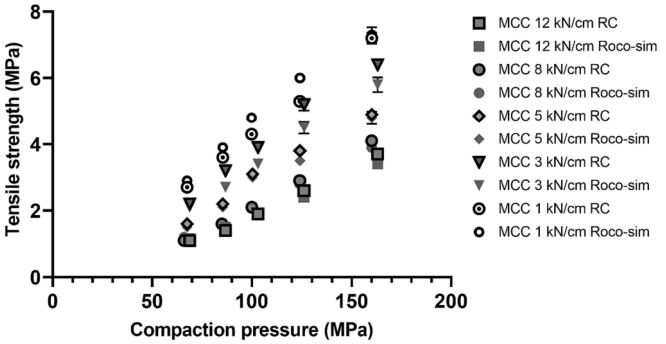

Fig. 5. Tabletability profile of MCC produced by compaction simulator and oscillating and roller compactor at increasing compaction forces (n = 10) (mean ± SD).

mimic the compaction process of a roller compactor to produce tablet-like ribbons known as riblets.

Several studies have utilized uniaxial compaction to simulate the roller compaction process (Zinchuk et al., 2004; Reimer and Kleinebudde, 2019; Gupta et al., 2005). The studies are based on the thin layer model, which assumes that the material between the rolls of a roller compactor can be separated into thin powder layers of constant width equal to the roll width, with a constant height, length, and mass equal to the three-dimensional volume of the thin layer. This means that the relative density of a layer depends only on the applied force and the relative layer length corresponding to the roll gap width. The transfer between equipment based on ribbon relative density is a well-known development strategy (Peter et al., 2010; Rowe et al., 2017). Previous studies have utilized a compaction simulator to simulate a roller compaction process and showed that upon compression, over a range of specific compaction forces, the riblets and ribbons had similar relative densities and tensile strengths (Zinchuk et al., 2004; Gupta et al., 2005). In contrast, a recent study utilizing a MedelPharm Styl'One Evolution compaction simulator to simulate a Gerteis Mini-pactor roller compactor showed an increased relative density of the riblets produced by the compaction simulator compared to the ribbons produced by the roller compactor when simulating compaction at a gap of 2 or 4 mm between 5 and 15 kN/cm. Therefore, a correction factor [Kp] was proposed to adjust the applied force of the compaction simulator with a factor of 0.67 to obtain the same relative density of the riblets and ribbons. However, the study did not investigate the compression of granulated riblets into tablets and this is a common drawback in studies to date (Reimer and Kleinebudde, 2019). In most cases, tablets will be the final dosage form and understanding the influence of granule properties on tablet properties is key to assessing this approach to roller compaction method development. The aim of this study is therefore to investigate the feasibility of a compaction simulator and an oscillating mill to mimic the complete roller compaction process in a material sparing way and to further compress the respective granules into tablets to understand the influence of the two different preparation methods on tablet mechanical properties. Microcrystalline cellulose (MCC) and dicalcium phosphate dihydrate (DCPD) were selected as raw materials to represent soft, ductile materials that undergo plastic deformation and hard, brittle materials that tend to undergo fragmentation, respectively.

2. Materials and methods

2.1. Materials

Microcrystalline cellulose (Avicel PH102) was obtained from FMC (Philadelphia, PA, United States), dicalcium phosphate dihydrate (Emcompress Premium) was obtained from Rettenmaier (Holstebro,

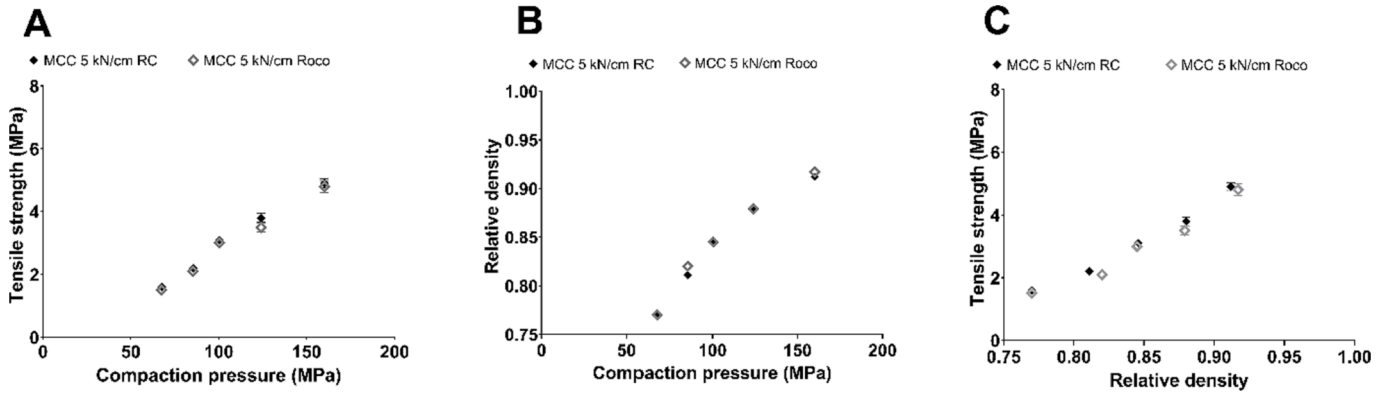

Fig. 6. Tabletability (A), compressibility (B) and compactability (C) of MCC produced by compaction simulator and roller compactor at 5 kN/cm (n = 10) mean ± SD.

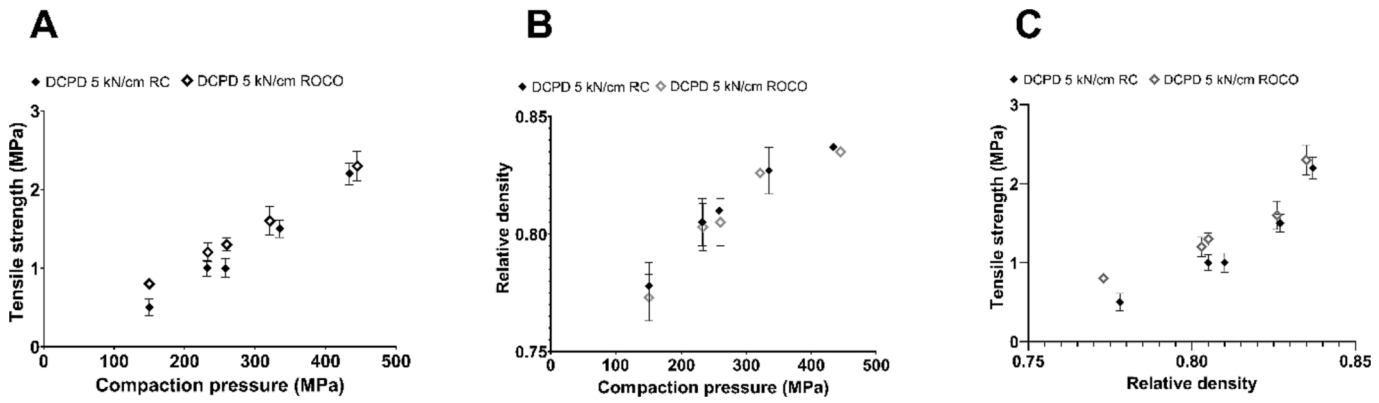

Fig. 7. Tabletability (A), compressibility (B) and compactability (C) of DCPD compaction profiles produced by compaction simulator and roller compactor at 5 kN/cm (n = 10) (mean ± SD).

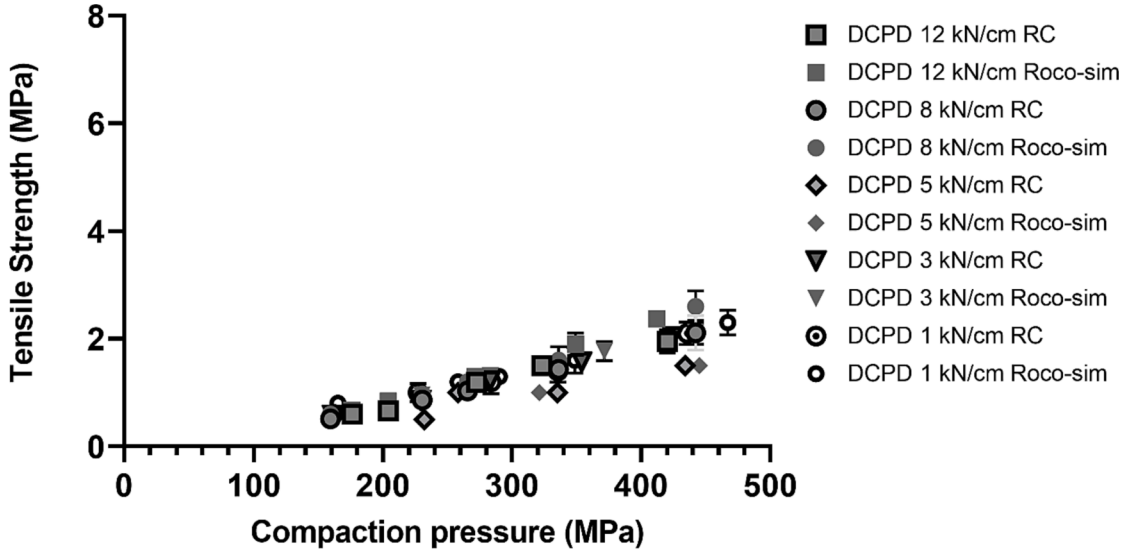

Fig. 8. Tabletability profile of DCPD produced by compaction simulator and roller compactor at increasing specific compaction forces.

Table 1
Overview of material consumption.

	Compaction simulator	Roller compaction
Parameter setup (g)	<5	<10
Feeder dead volume (g)	<20	<100
Waste in equipment (g)	<5	<5
Mill dead volume (g)	<10	<5
Total (g)	<40	<120

Denmark) and magnesium stearate (Ligamed MF-2-V) was obtained from Peter Greven (Bad Münstereifel, Germany). The materials were used as received, however DCPD was mixed with 1% w/w magnesium stearate to avoid adhesion in the equipment whereas lubrication could be avoided when using MCC.

2.2. Manufacturing of ribbons

Ribbons were manufactured using a roller compactor. A Gerteis Mini-polygran (Rapperswil-Jona, Switzerland) was equipped with 15 cm rolls with a width of 2.5 cm. A roll gap of 2 mm was applied using gap control and the roll speed was kept at 1 rpm. The specific compaction force was set at 1, 3, 5, 8 or 12 kN/cm. Ribbons were collected for each specific compaction force.

2.3. Milling of ribbons

The ribbons were milled by a star granulator in the Gerteis Mini-polygran roller compactor (Rapperswil-Jona, Switzerland). The granulator was set at 17 rpm clockwise rotation and 50 rpm counterclockwise rotation at an angle of 100 and 900 degrees, corresponding to 0.28 and 2.5 complete rotations of the star granulator, respectively. A 0.8 mm conidur screen was used with 0.8 mm spacers. Granules were collected from each milling of ribbons produced as described in section 2.2.

2.4. Manufacturing of riblets

Riblets were manufactured using a compaction simulator. A Medel-Pharm Styl'One Evolution (Beynost, France) was equipped with 10 x 20 mm rectangular flat-face punches. The simulated roll speed was set at 1 rpm and the simulated specific compaction force was set at a compaction pressure equal to 1, 3, 5, 8 or 12 kN/cm at a gap of 2 mm. A gravity feeder was used, the correction factor Kp was set at 1.0 and the overfill was set at 0 mm. Riblets were collected for each compaction pressure.

2.5. Milling of riblets

The riblets were milled using an oscillating mill. The riblets were added to a Frewitt OscilloWitt-Lab (Granges-Paccot, Switzerland). For

Table A1
Summary of size distributions of MCC and DCPD as received and after granulation by the oscillating mill or star granulator.

Material	Millling equipment	Specific Compaction Force (kN/cm)	Dx (10) (μm)	Dx (50) (μm)	Dx (90) (μm)	Span (μm)
DCPD	As received	NA	118	228	390	1.192
DCPD	OM	1	8.03	93.5	280	2.907
DCPD	SG	1	6.21	95.7	291	2.975
DCPD	OM	3	7.75	114	546	1.505
DCPD	SG	3	5.83	96.3	453	1.508
DCPD	OM	5	8.60	243	1030	4.202
DCPD	SG	5	5.68	114	658	5.736
DCPD	OM	8	13.3	577	1590	2.728
DCPD	SG	8	7.09	225	896	3.957
DCPD	OM	12	21.2	606	1430	2.318
DCPD	SG	12	8.23	301	951	290.5
MCC	As received	NA	32.6	107	239	1.924
MCC	OM	1	35.0	118	298	2.222
MCC	SG	1	37.8	121	318	2.309
MCC	OM	3	57.5	242	903	3.491
MCC	SG	3	43.4	162	638	3.665
MCC	OM	5	62.6	337	1000	2.788
MCC	SG	5	49.5	208	791	3.572
MCC	OM	8	64.3	364	1010	2.586
MCC	SG	8	56.1	283	861	2.844
MCC	OM	12	86.4	451	1060	2.161
MCC	SG	12	59.3	293	875	2.780

*SG = star granulator, OM = oscillating mill.

MCC, a speed of 1200 mm/s was applied. For DCPD a speed of 300 mm/s was applied. The gap was set at 4 (arbitrary scale) corresponding to approx. 0.8 mm and a conidur 0.8 mm screen was used. Granules were collected from each milling of riblets produced as described in section 2.4.

2.6. Pycnometry

The apparent density of ribbons and riblets was determined using pycnometry. The ribbons and riblets were cut into rectangular pieces of approximately 1 × 1 cm corresponding to a sample mass of 0.2–0.5 g. The mass of each sample was determined with a Mettler Toledo high precision balance (Glostrup, Denmark). The envelope density of the samples was determined using a Micromeritics Geopyc 1365 (Norcross, GA, USA). The internal diameter tube, consolidation force and conversion factor of 12.7 mm, 28 N and 0.1284 cm^3/mm, respectively were used. The experiment was conducted in triplicate.

2.7. Laser diffraction

The granule size distribution was determined using laser diffraction. Laser diffraction was performed using a Malvern Panalytical Mastersizer 3000 (Malvern, Great Britain). Approx. 3 g of sample was measured using an Aero S automated dry powder dispersion unit at pressure 1 bar at a feed rate of 50%. The particle size distribution was calculated based on the detected scattering pattern from which the volume of the particle is calculated and then transformed to equivalent sphere diameter. The experiment was conducted in duplicate.

2.8. Scanning electron microscopy

Morphology of the granules was determined using scanning electron microscopy. The samples were dispersed on carbon tape and sputter coated with gold for 90 min using a 16 nm, MSC1T, LOT-QuantumDesign (Darmstadt, Germany). Images were acquired using a ThermoFisher Fei Quanta 250 (Karlsruhe, Germany) at a magnification level of 100–500.

2.9. Manufacturing of tablets

Tablets were manufactured using a compaction simulator. A MedelPharm Styl'One Evolution (Beynost, France) was equipped with a 10 mm flat face punch for MCC to produce tablets 400 mg. To reduce consumption for a material sparing approach, a 6 mm flat face punch was used for DCPD to produce tablets of 200 mg. The tablet press was equipped with a force feeder with pins operating at 10%. The press simulated a Fette 102i at a speed of 20 rpm. Tablets were produced in the range of 50 to 500 MPa. Before use, the punch deformation was determined using the operating software Analis (Beynost, France).

2.10. Tablet mass, height, breaking force, true density and relative density

The mass of 10 tablets was determined using a Mettler Toledo high precision balance (Glostrup, Denmark). The height and breaking force of 10 tablets were determined using an Erweka TBH 425 tablet hardness tester (Langen, Germany). The tablet tensile strength σ is derived from the breaking force using Eq. (1):

$$\sigma = 2F/\pi dh \quad (1)$$

where F is the breaking force, d is the tablet diameter and h is the tablet height.

The relative density of ribbons, riblets and tablets was derived using Eq. (2):

$$Relative\ density = Apparent\ density / True\ density \quad (2)$$

The true density of MCC (1.58 g/cm^3) and DCPD (2.56 g/cm^3) was determined by helium pycnometry using a Micromeritics Accupyc II 1340 (Brussels, Belgium).

3. Results and discussion

3.1. Characterization of ribbons and riblets

The relative density of ribbons and riblets produced using a roller compactor and compaction simulator, respectively, was investigated using pycnometry to determine the correction factor Kp (Reimer and Kleinebudde, 2019). The ribbons and riblets were produced at specific compaction forces between 1 and 12 kN/cm and, as expected, their respective relative density increases with increasing specific compaction force as shown in Figure 1. Across all applied forces, the relative density of the ribbons and riblets showed no statistically significant difference ($p > 0.01$), independent of the raw material used (Figure 1). This means that a Kp of 1 is required to simulate the Gerteis Mini-polygran roller compactor when using the MedelPharm Styl'One Evolution compaction simulator. In turn, this also means that the compaction simulator adequately mimics the uniaxial compression of the roller compactor as originally proposed based on the thin layer model (Peter et al., 2010). This has also been shown in a previous study, which attempted to mimic the Gerteis Mini-pactor using the same compaction simulator and found a Kp factor of 0.67 was required (Reimer and Kleinebudde, 2019). The study also concluded that the Kp factor is machine dependent, but material independent, which is in line with findings in the current study. As seen in Figure 1, the relative density of riblets produced from MCC and DCPD at a specific compaction force of 8 and 12 kN/cm plateau and show higher variation. This can be explained by over-compression of the material, which can result in lamination of the riblet and in turn in uneven density. This is a well-known phenomenon of roller compaction when compacting material at high forces (Sun and Sun, 2017; Wiedey and Kleinebudde, 2017). Furthermore, this may lead to an underestimation of the blend properties as an increasing ribbon density may result in a lower amount of small particles during milling, which can significantly increase blend flowability and decrease tablet tensile strength (Sakwanichol et al., 2012).

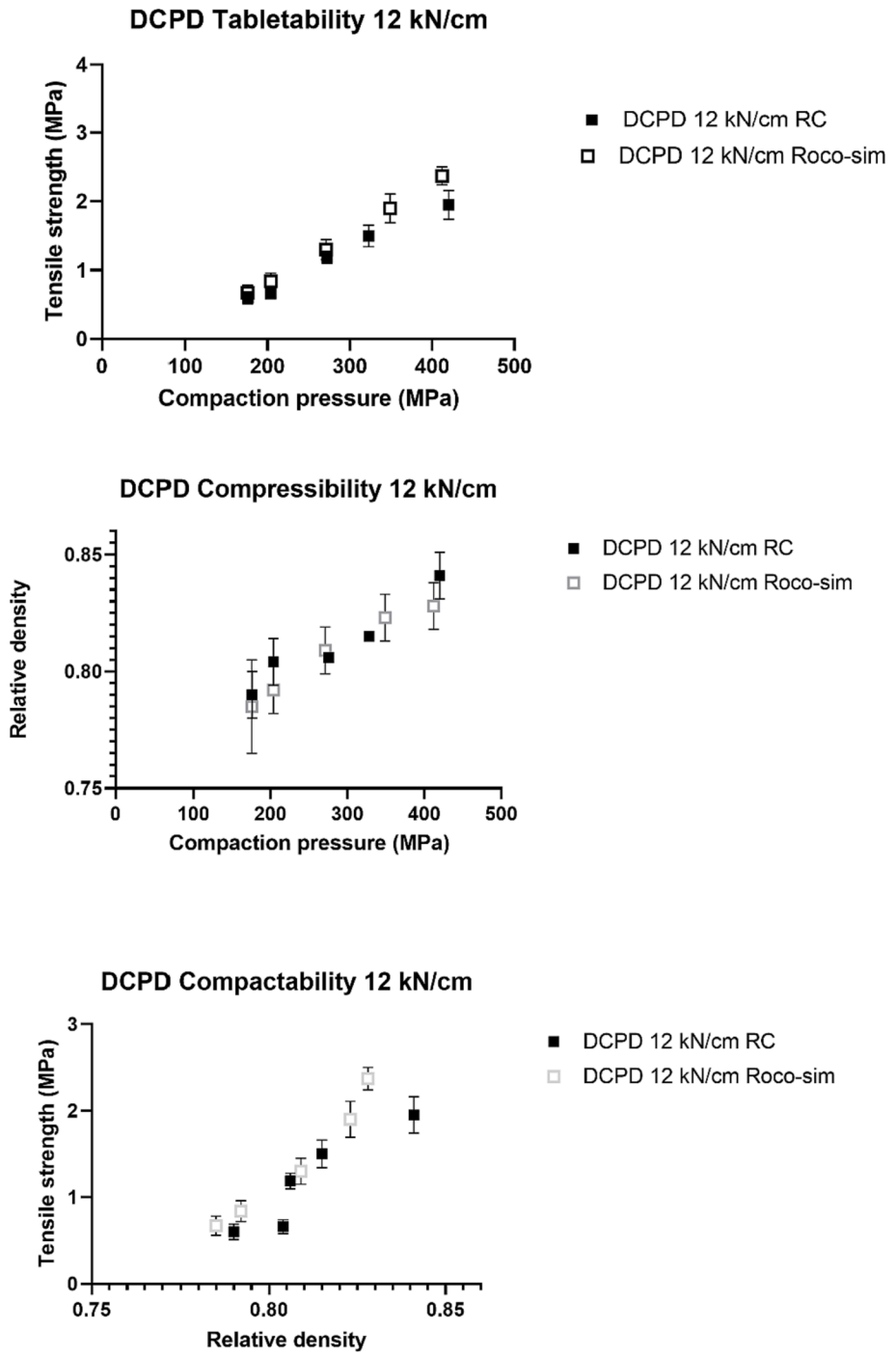

Fig. B1. DCPD compaction profiles produced by compaction simulator and roller compactor at 12 kN/cm (n = 10) (mean ± SD).

3.2. Characterization of granules

The morphology and particle size distribution (PSD) of the raw materials and granules were investigated to determine the ability of the compaction simulator and oscillating mill to mimic the roller compactor and star granulator. MCC, as received, appeared as agglomerates of crystallites, while DCPD, as received, appeared as fused prismatic particles as shown in Figure 2. Upon roller compaction, the MCC particles formed larger agglomerates, while the DCPD particles appear to have an increased in surface roughness. This behaviour on milling is expected from the soft, ductile nature of MCC and the hard, brittle nature of DCPD (Roberts and Rowe, 1987). Critically, the compaction simulator and roller compactor granule morphologies appear indistinguishable by scanning electron microscopy.

Milling parameters such as gap, speed, and sieve design as well as material properties can have a significant influence on final granule properties (Perez-Gandarillas et al., 2016). Granules of MCC and DCPD prepared by the star granulator and the oscillating mill resulted in similar PSDs, respectively, as shown in Figure 3 and Appendix A. All the granules produced showed bimodal PSD independent of milling equipment. For MCC, the smaller peak is at the approximately the same size class as the received material. For DCPD, the main peak in the PSD of the granules from the star granulator overlaps the position for the as received material. In general, there was a higher level of smaller

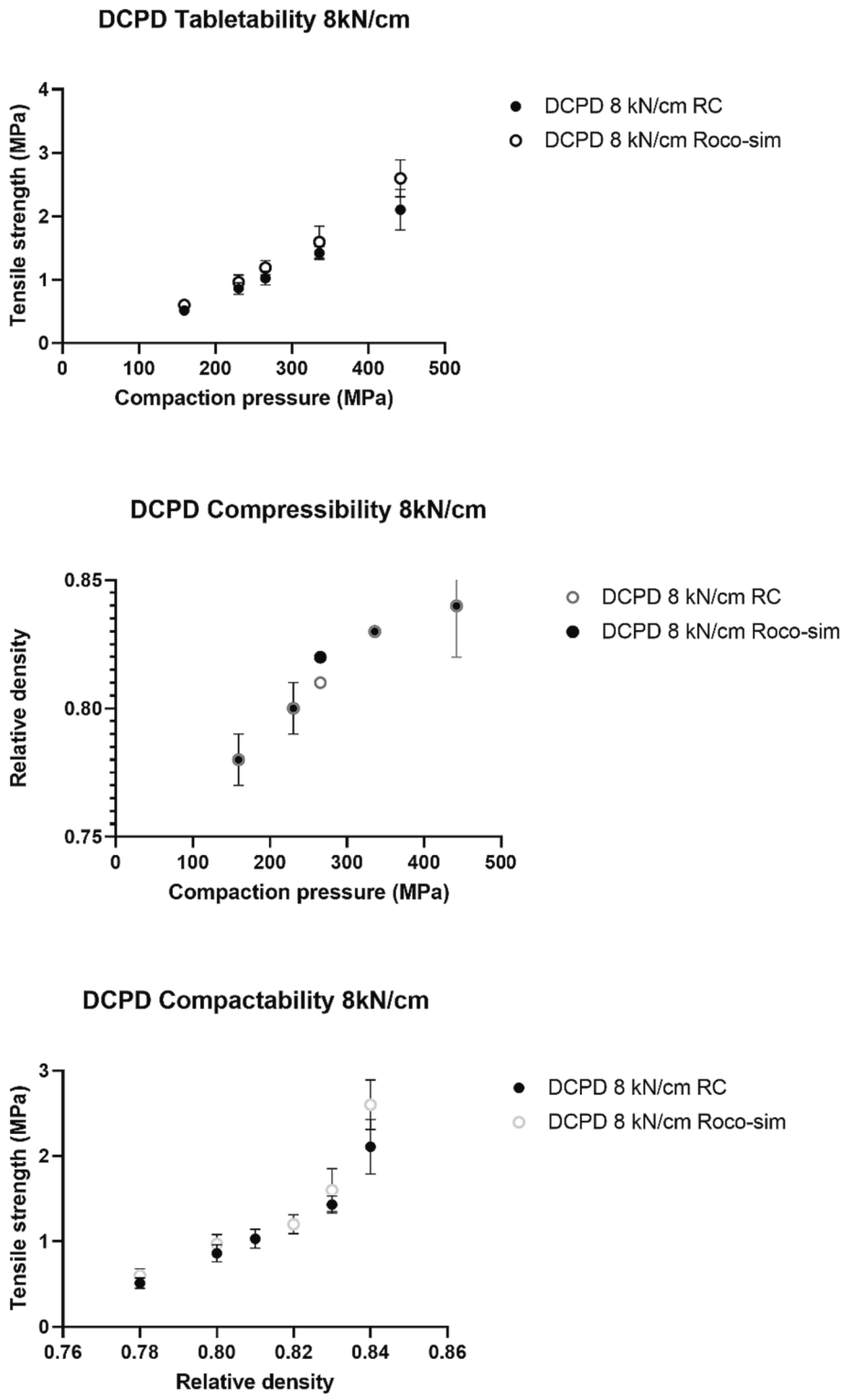

Fig. B2. DCPD compaction profiles produced by compaction simulator and roller compactor at 8 kN/cm (n = 10) (mean ± SD).

particles with DCPD when compared to MCC following granulation. While this particle size reduction seen for DCPD is not the normal aim of granulation, it is useful that compaction simulation can mimic this behaviour. For both ductile and brittle materials, the PSD obtained from a traditional roller compactor can be conveniently reproduced using a compaction simulator and oscillating mill.

Specific compaction force is a critical process parameter of roller compaction and its impact on granule PSD is summarised in Figure 4 and Appendix A. Increasing specific compaction force results in an increased ribbon density, which can lead to increased ribbon tensile strength and subsequently a narrower PSD (Sakwanichol et al., 2012). For MCC, as the specific compaction force is increased the PSD shifted towards larger particle sizes. This can be seen in the smaller particle size peak of the bimodal distribution. For the 1 kN/cm granules, this peak closely resembled the peak for the as received material. As the specific compaction force is increased, this peak decreased until it appeared as a

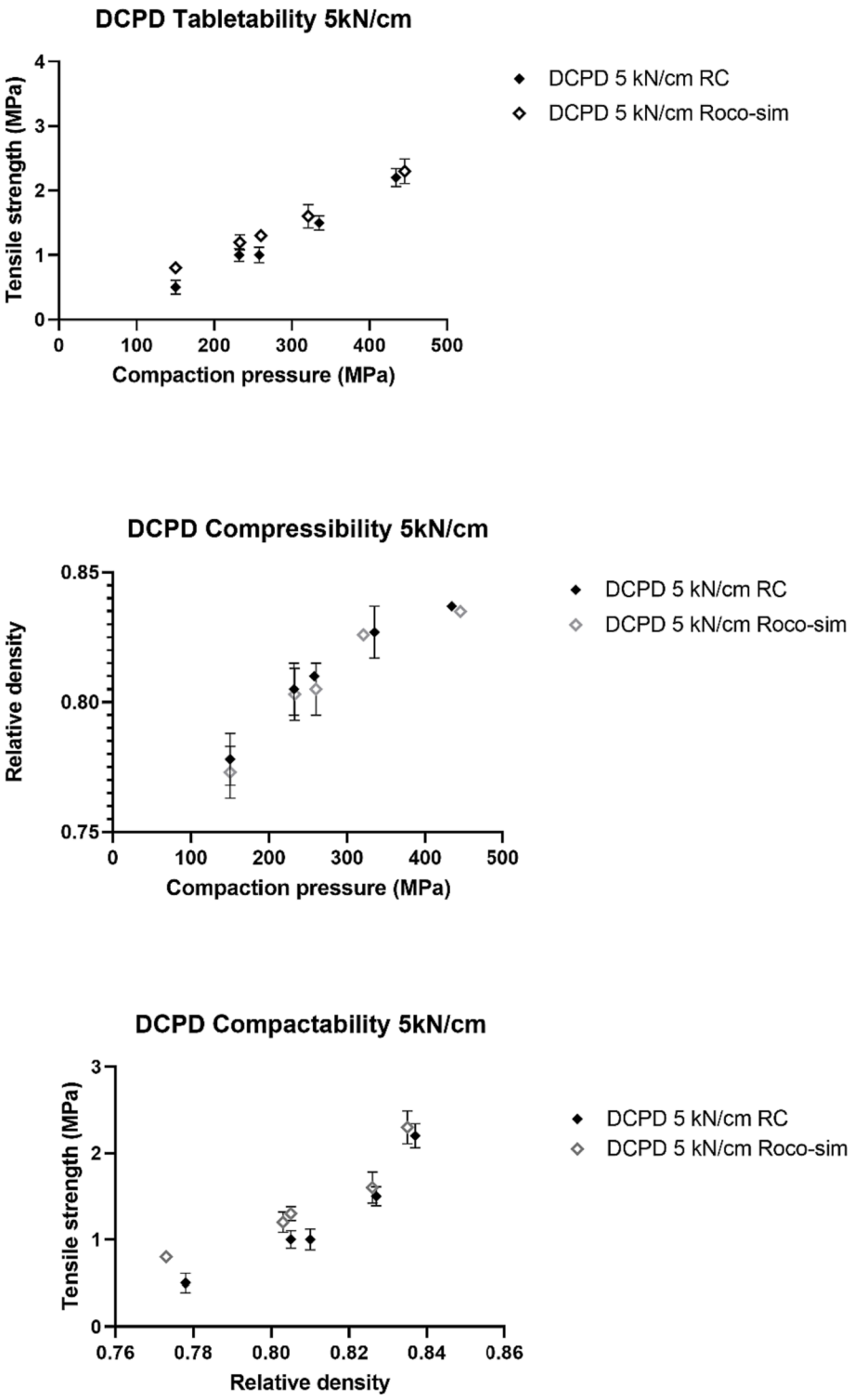

Fig. B3. DCPD compaction profiles produced by compaction simulator and roller compactor at 5 kN/cm (n = 10) (mean ± SD).

small shoulder peak for the 12 kN/cm granules. For DCPD, there was a similar shift in the PSDs towards larger particle sizes with increasing specific compaction forces, with main peak moving to a larger size class and the smaller size class peak diminishing. Furthermore, for all specific compaction forces, the granulation process resulted in higher level of small particles compared to DCPD as received.

3.3. Characterization of tablets

The tabletability, compressibility and compactability of granules produced by the compaction simulator and the roller compactor were investigated. The tensile strength of the produced tablets increased with increasing compaction pressure independent of the material used as expected (Malkowska and Khan, 1983; Juban et al., 2017). For MCC, the tabletability was similar between the tablets from granules produced by the compaction simulator and oscillating mill and tablets from granules

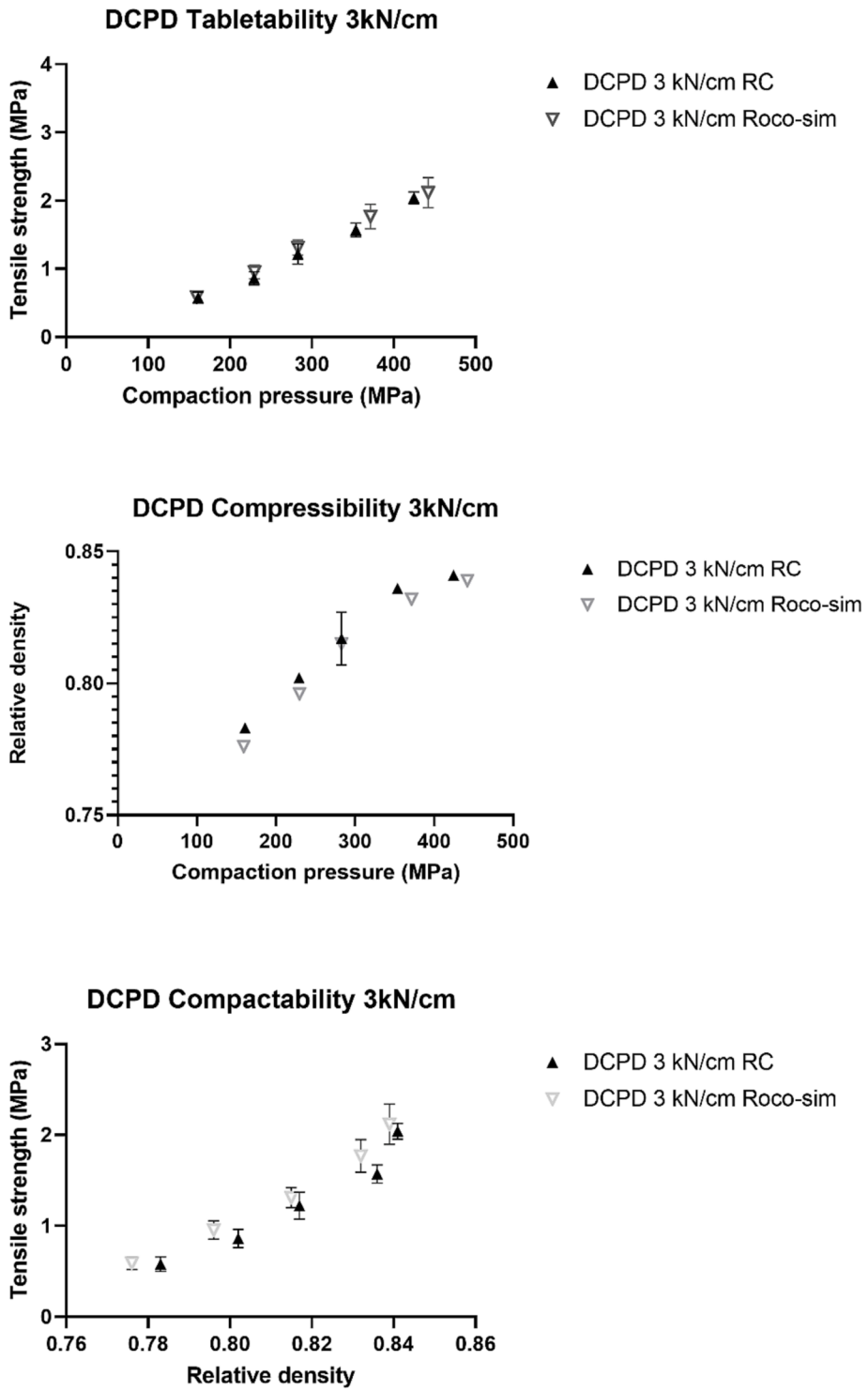

Fig. B4. DCPD compaction profiles produced by compaction simulator and roller compactor at 3 kN/cm (n = 10) (mean ± SD).

produced by the roller compactor as seen in Figure 6. This can be explained by the similarity in morphology and PSD between the two differently produced granules as shown in Figure 2 and Figure 3. Furthermore, the compactability and compressibility of tablets were similar independent of the granulation method, which can be attributed to the similar level of small particles filling void spaces in the compact and thereby creating interparticle interactions (Casian et al., 2022). Furthermore, the similar compressibility can be attributed to the particle morphology and ribbon relative density being similar (Hancock et al., 2003; Casian et al., 2022). Finally, there is also an effect of work hardening of MCC as shown with the decreasing tablet tensile strength as the specific compaction force increased (Figure 5). This may be a result of the initial stronger bonds breaking and reformation causing weaker bonding on re-compression (Malkowska and Khan, 1983; Juban et al., 2017).

For DCPD, the tabletability, compactability and compressibility were also similar between the tablets from granules produced by the compaction simulator and oscillating mill and tablets from granules produced by the roller compactor as seen in Figure 7. Again, this can be explained by the morphology and PSD of the two differently produced

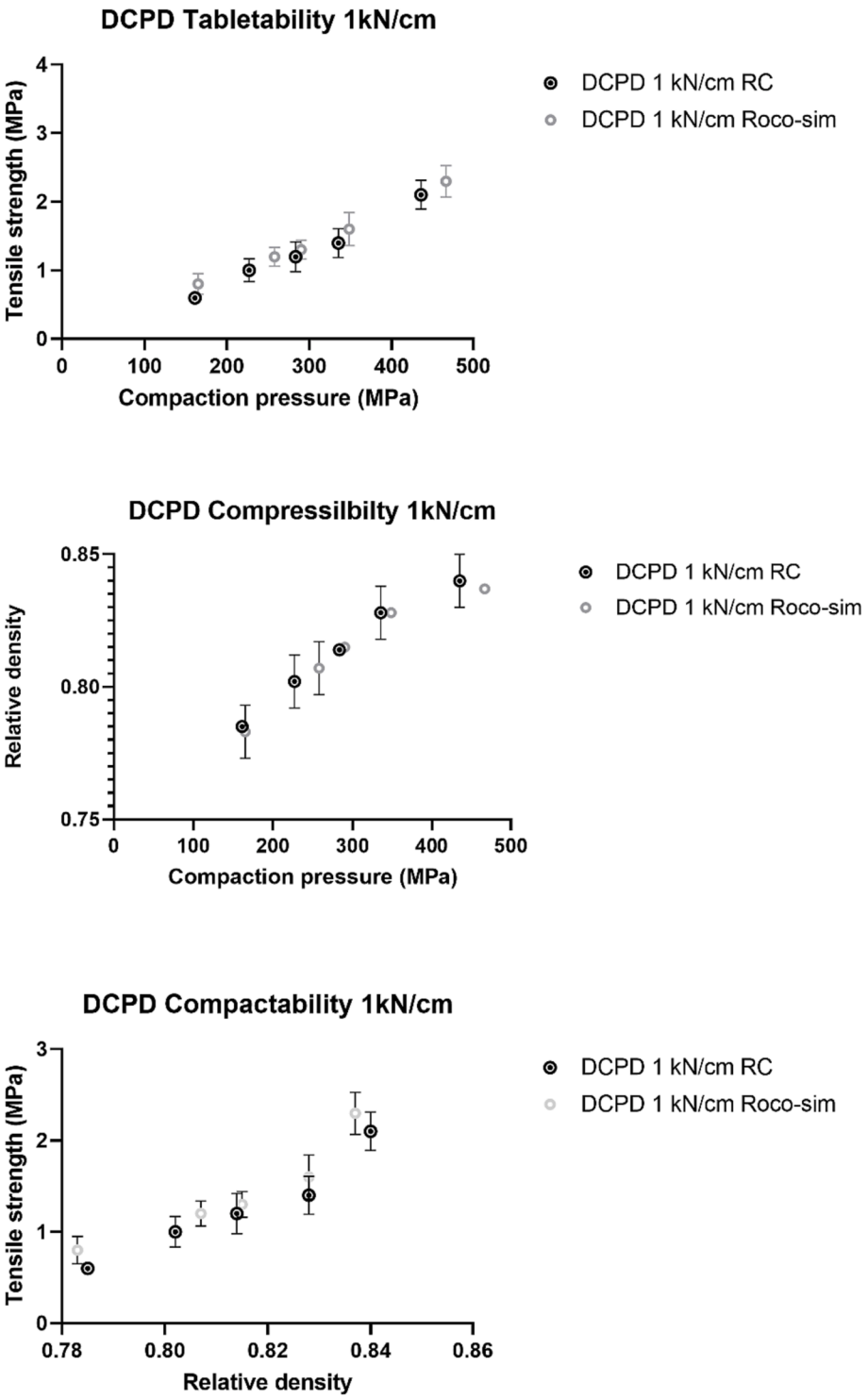

Fig. B5. DCPD compaction profiles produced by compaction simulator and roller compactor at 1 kN/cm (n = 10) (mean ± SD).

granules which were similar as shown in Figure 2 and Figure 3. These results were independent of the applied compaction pressure during tableting as shown in compaction profiles in Appendix B. In contrast to MCC, increasing specific compaction force used during roller compaction and roller compaction simulation, the tabletability of DCPD tablets remains relatively similar, which demonstrates the reworkability of brittle material, as shown in Figure 8. As the granules are compacted, bonds are broken, and fresh surfaces are available to make new bonds resulting in relatively unaffected rework potential (Iyer et al., 2014; Wu and Sun, 2007).

3.4. Roller compaction simulation as a material sparing method

The process development and scale-up of roller compaction to determine the specific compaction force, roll gap width, and roll speed, have historically relied upon large experimental designs or a trial-and-error approach, both of which can be material and time consuming. The lower material usage of the compaction simulator process is summarized in Table 1. While varying process parameters, the lower material usage in the compaction simulator was mainly driven by the slower throughput of the compaction simulator, the ease of changing the

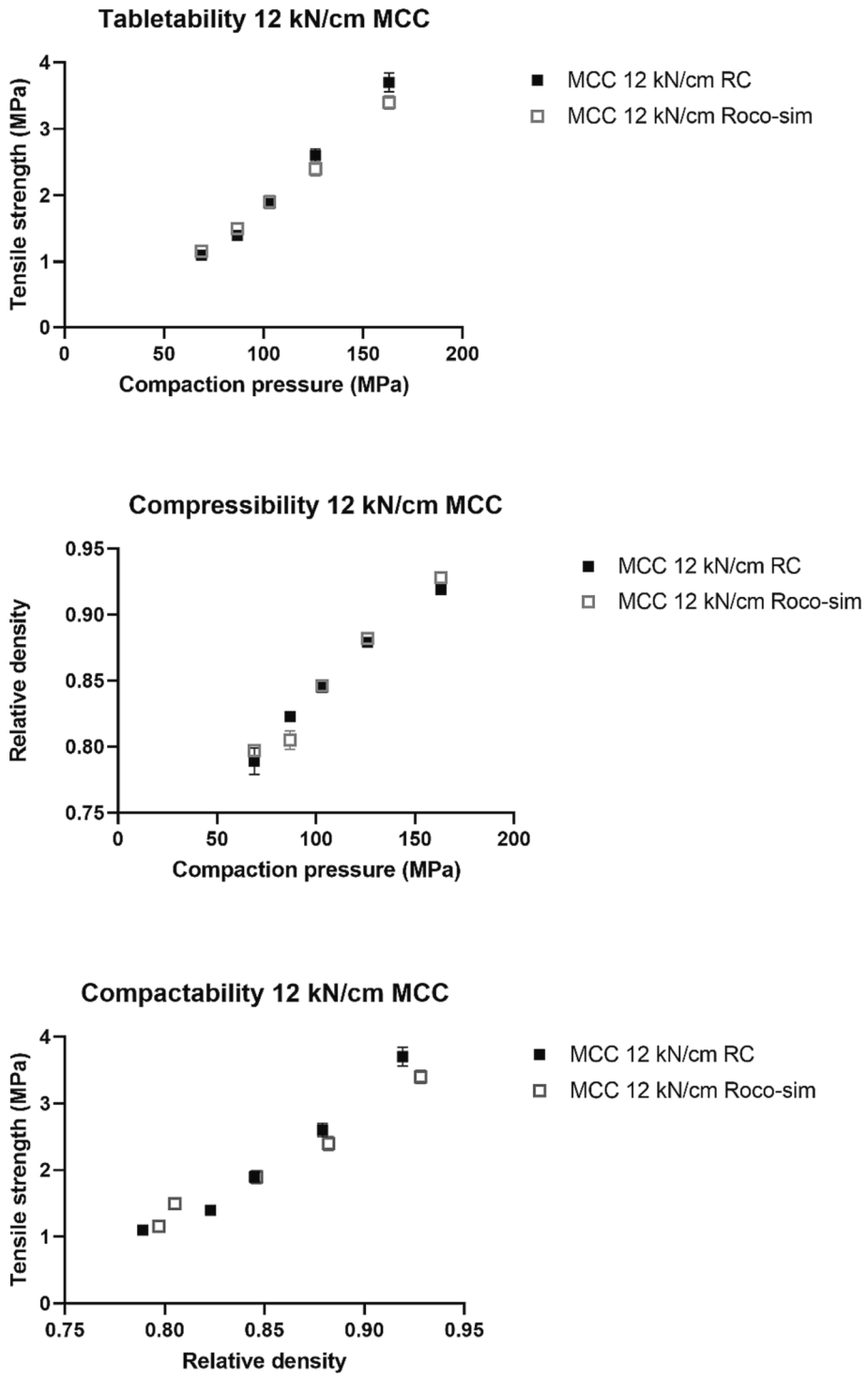

Fig. B6. MCC compaction profiles produced by compaction simulator and roller compactor at 12 kN/cm (n = 10) (mean ± SD).

process and speed to obtain steady state. For a single manufacturing run, the compaction simulator approach also resulted in significantly less material consumption, mainly driven by the lower dead volume in the feeder as shown in Table 1.

Ultimately, the work presented in this study demonstrates that the compaction simulator can adequately mimic the uniaxial compression of the roller compactor. Furthermore, that the oscillating mill can adequately mimic the roller compactor star granulator and that the produced tablets showed similar mechanical properties for both soft and hard materials. The implementation of compaction simulation resulted in considerable material and time savings during drug product development.

4. Conclusion

The feasibility of using a compaction simulator and oscillating mill to mimic a roller compactor was investigated in this study using MCC and DCPD as raw materials. Pycnometry of riblets produced by the use of the compaction simulator and ribbons produced by the use of the roller compactor showed similar relative density independent of raw material

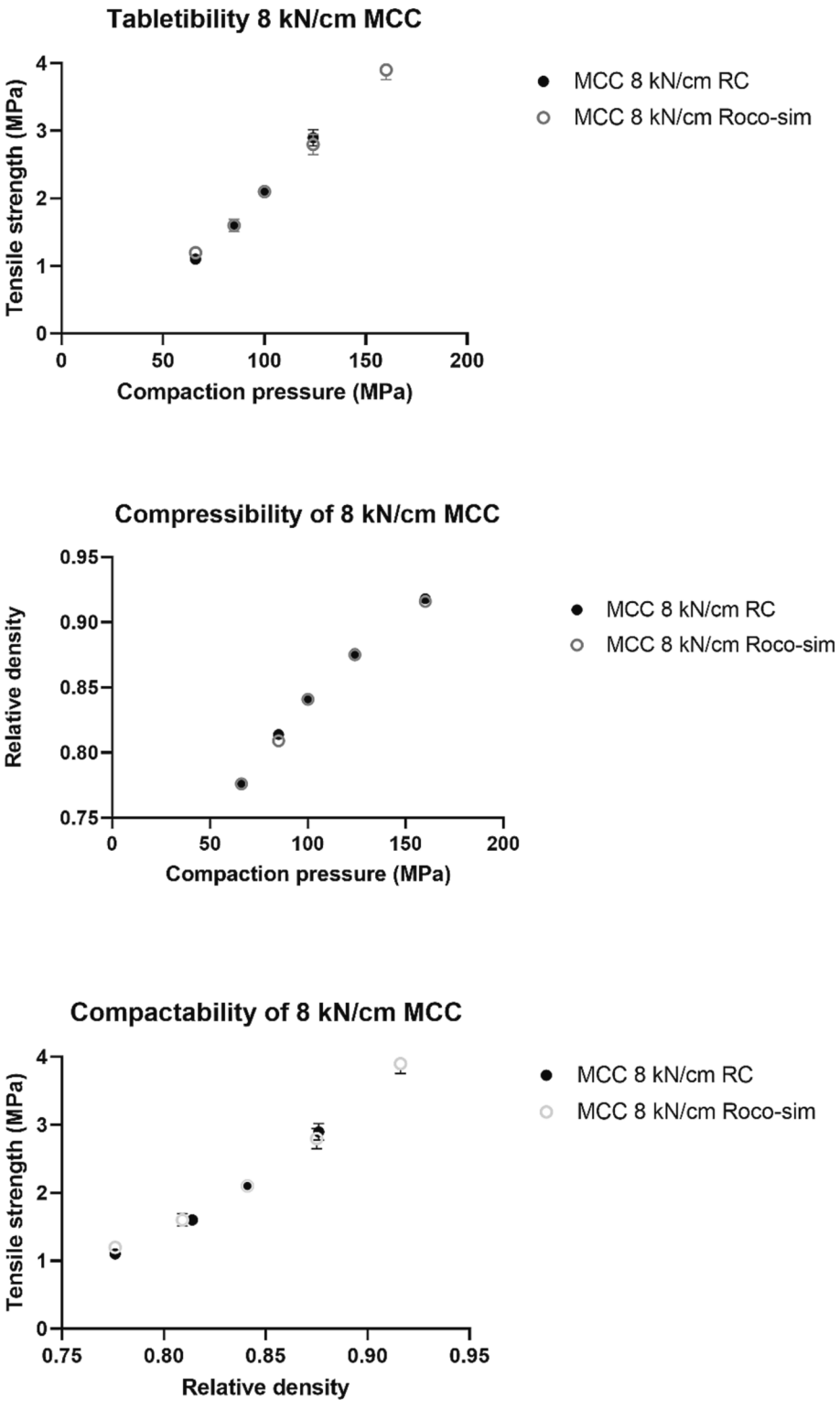

Fig. B7. MCC compaction profiles produced by compaction simulator and roller compactor at 8 kN/cm (n = 10) (mean ± SD).

between 1 and 12 kN/cm, which means that the compaction simulator adequately mimics the compaction of the roller compactor. Scanning electron microscopy of the granules produced by the use of the oscillating mill and star granulator showed similar morphology and laser diffraction of the same respective granules showed similar PSD, which means that the oscillating mill adequately mimics the star granulator when matching gap and sieve design. The tabletability, compressibility and compactability of the respective granules were also shown to be similar further demonstrating that compaction simulator in combination with oscillating mill adequately mimics the roller compactor for both soft and hard materials. Finally, a significant amount of material and time was saved using a compaction simulator in combination with an oscillating mill compared to the roller compactor.

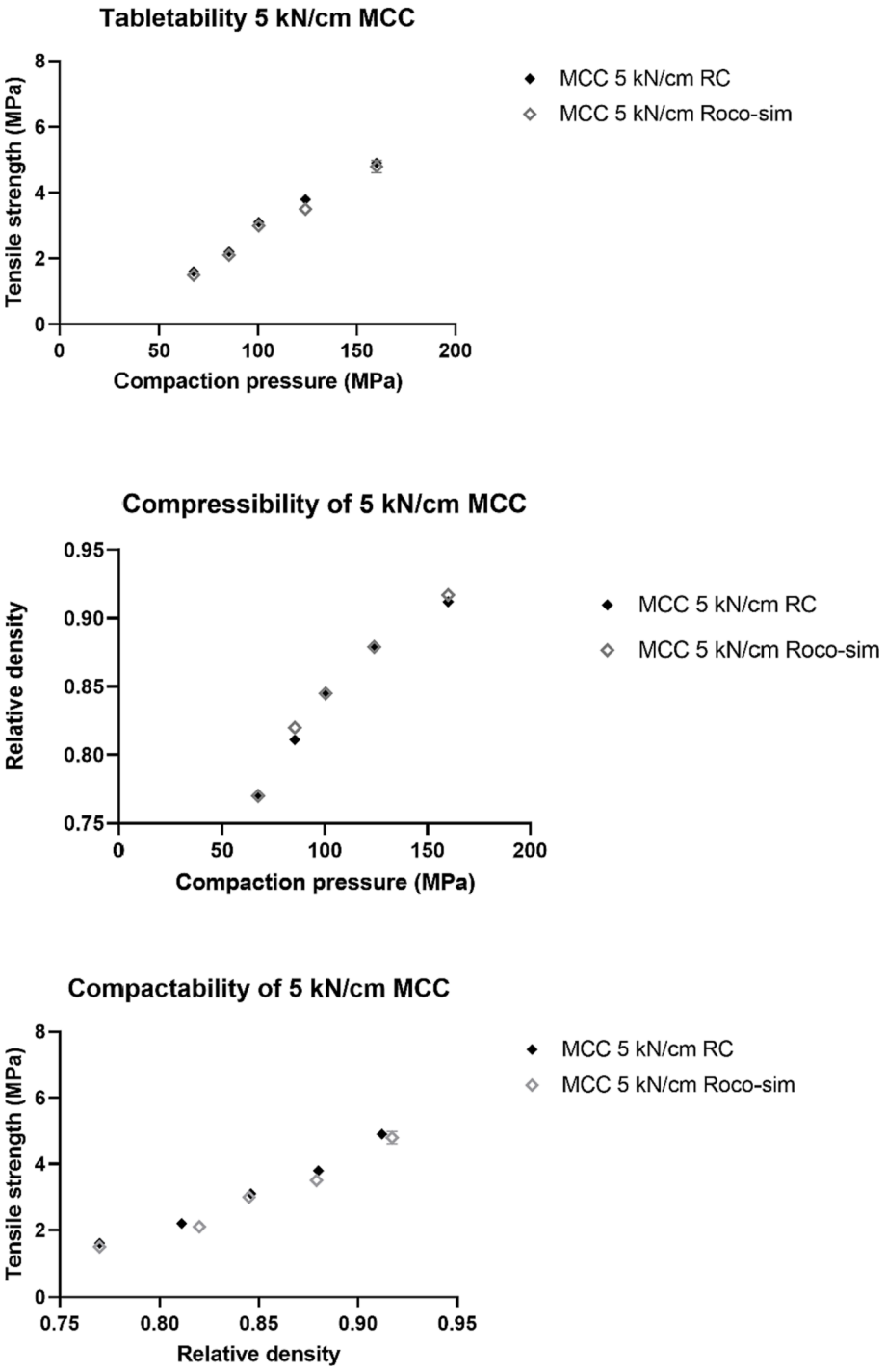

Fig. B8. MCC compaction profiles produced by compaction simulator and roller compactor at 5 kN/cm (n = 10) (mean ± SD).

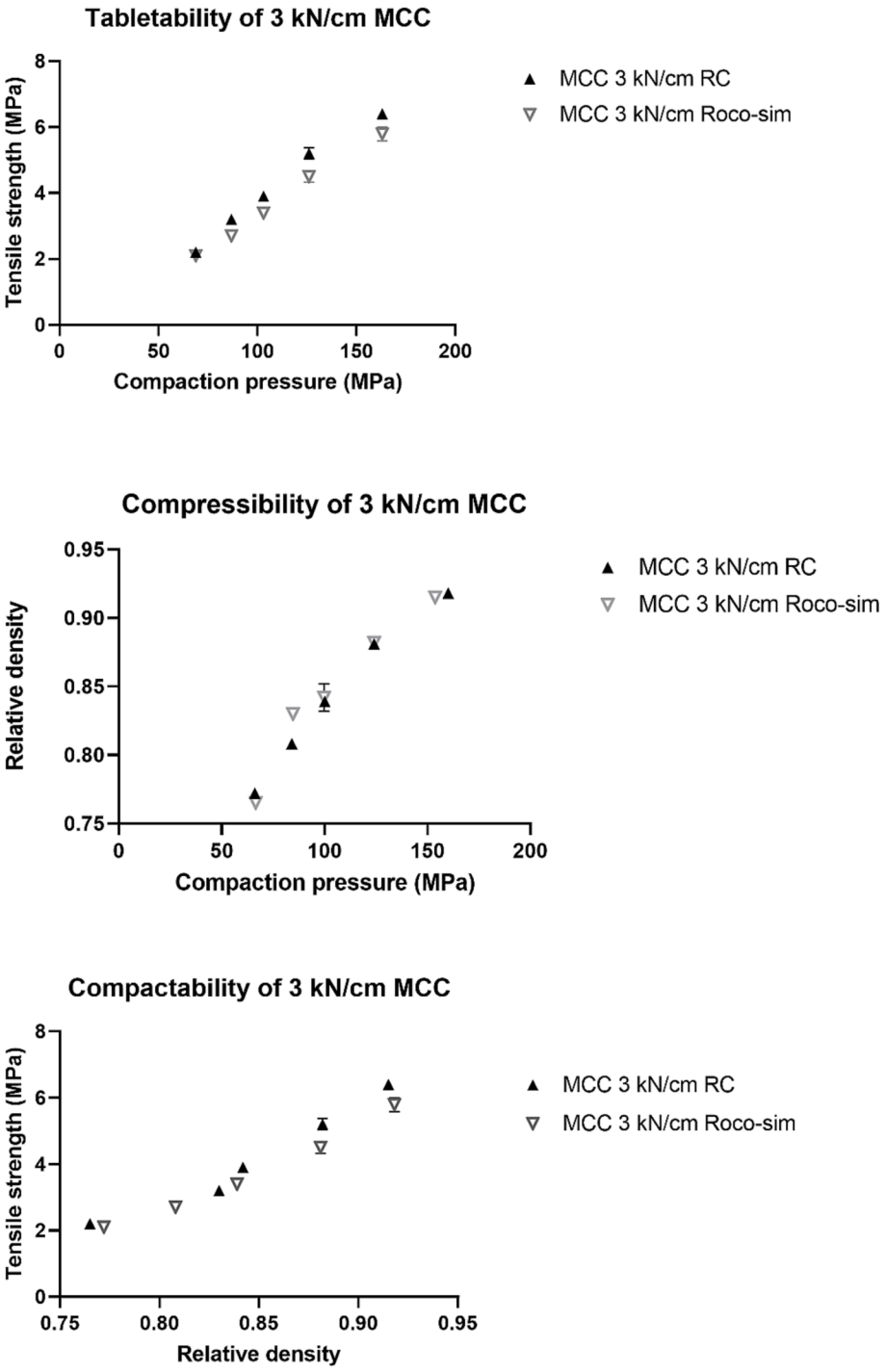

Fig. B9. MCC compaction profiles produced by compaction simulator and roller compactor at 3 kN/cm (n = 10) (mean ± SD).

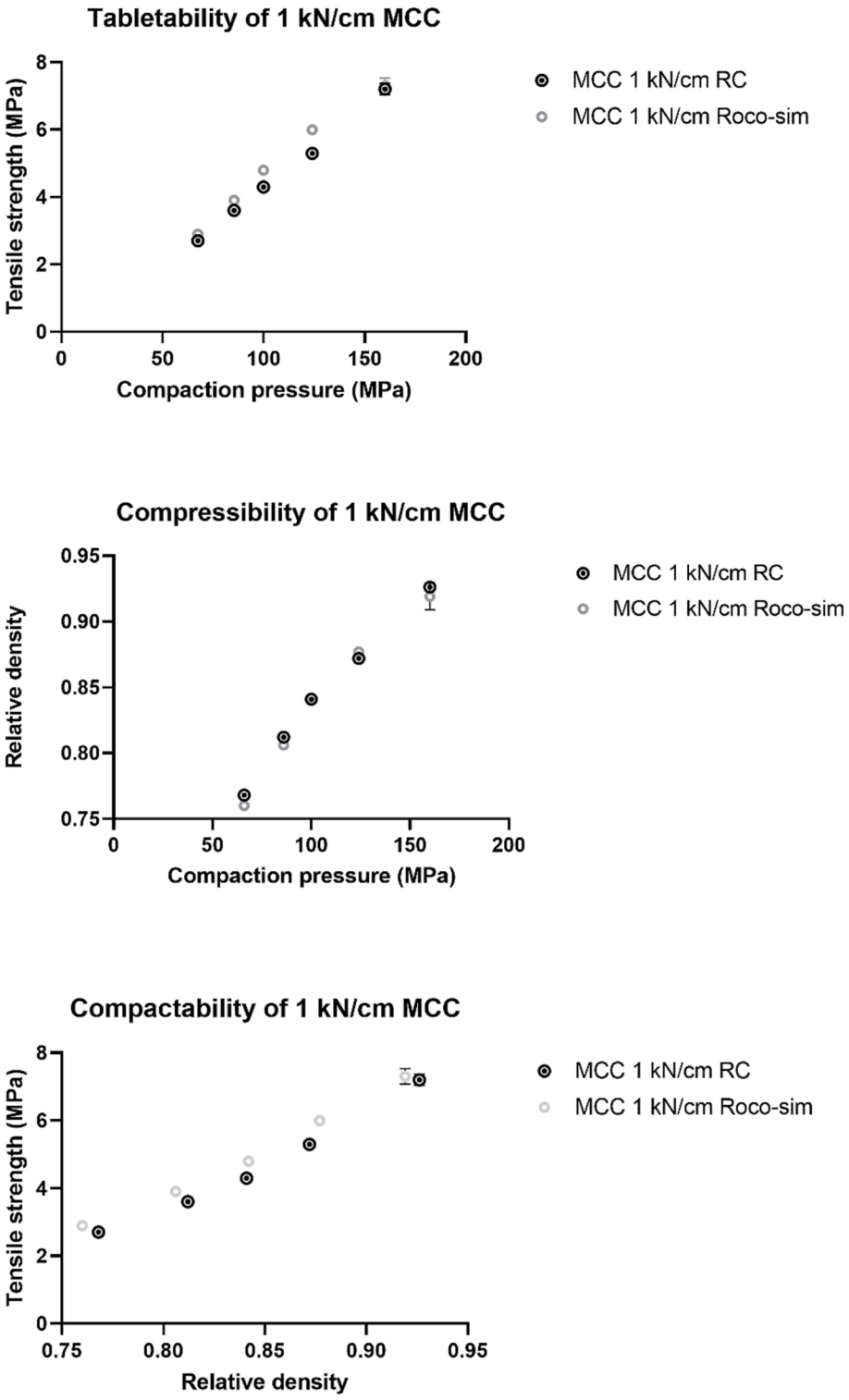

Fig. B10. MCC compaction profiles produced by compaction simulator and roller compactor at 1 kN/cm (n = 10) (mean ± SD).

CRediT authorship contribution statement

Layla Hassan: Data curation, Formal analysis, Investigation, Writing – original draft. **René Jensen:** Data curation, Formal analysis, Investigation, Writing – original draft. **Andrew Megarry:** Conceptualization, Formal analysis, Supervision, Writing – original draft, Writing – review & editing. **Lasse I. Blaabjerg:** Conceptualization, Formal analysis, Investigation, Supervision, Writing – original draft, Writing – review & editing.

Declaration of Competing Interest

The authors declare that they have no known competing financial interests or personal relationships that could have appeared to influence the work reported in this paper.

Data availability

Data will be made available on request.

Acknowledgements

The authors would like to thank Susanne Bjerggaard Juul-Mortensen from Novo Nordisk, Denmark, for assistance with the acquisition of the laser diffraction and scanning electron microscopy results used in this study.

Appendix A

See the Table A1.

Appendix B

See the fig B1 to B10.

References

Bultmann, J.M., 2002. Multiple compaction of microcrystalline cellulose in a roller compactor. Eur. J. Pharm. Biopharm. 54 (1), 59–64. https://doi.org/10.1016/S0939-6411(02)00047-4.

Casian, T., Iurian, S., Gâvan, A., Porfire, A., Pop, A.L., Crișan, S., Puşcaş, A.M., Tomuță, I., 2022. In-Depth Understanding of Granule Compression Behavior under Variable Raw Material and Processing Conditions. Pharmaceutics. 14 (1), 177. https://doi.org/10.3390/pharmaceutics14010177.

Gupta, A., Peck, G.E., Miller, R.W., Morris, K.R., 2005. Influence of Ambient Moisture on the Compaction Behavior of Microcrystalline Cellulose Powder Undergoing Uni-Axial Compression and Roller-Compaction: A Comparative Study Using Near-Infrared Spectroscopy. J. Pharm. Sci. 94 (10), 2301–2313. https://doi.org/10.1002/jps.20430.

Haeffler, G., Schmidt, L., Lakio, S., Reynolds, G., Ödman, J., Tajarobi, P., 2019. A systematic study of the impact of changes of roller compactor equipment on granule and tablet properties. Powder Technol. 341, 11–22. https://doi.org/10.1016/j.powtec.2018.09.002.

Hancock, B.C., Colvin, J., Mullarney, M.P., Zinchuk, A.V., 2003. The relative densities of pharmaceutical powders, blends, dry granulations, and immediate-release tablets. Pharm. Technol. 27, 64–80.

Iyer, R.M., Hegde, S., DiNunzio, J., Singhal, D., Malick, W., 2014. The impact of roller compaction and tablet compression on physicomechanical properties of pharmaceutical excipients. Pharm. Dev. Technol. 19 (5), 583–592. https://doi.org/10.3109/10837450.2013.813541.

Juban, A., Briançon, S., Puel, F., Hoc, T., Nouguier-Lehon, C., 2017. Experimental study of tensile strength of pharmaceutical tablets: effect of the diluent nature and compression pressure. EPJ Web Conf. 140, 13002. https://doi.org/10.1051/epjconf/201714013002.

Kleinebudde, P., 2022. Improving Process Understanding in Roll Compaction. J. Pharm. Sci. 111 (2), 552–558. https://doi.org/10.1016/j.xphs.2021.09.024.

Malkowska, S., Khan, K.A., 1983. Effect of Re-Conpression on the Properties of Tablets Prepared by Dry Granulation. Drug Dev. Ind. Pharm. 9 (3), 331–347. https://doi.org/10.3109/03639048309044678.

Perez-Gandarillas, L., Perez-Gago, A., Mazor, A., Kleinebudde, P., Lecoq, O., Michrafy, A., 2016. Effect of roll-compaction and milling conditions on granules and tablet properties. Eur. J. Pharm. Biopharm. 106, 38–49. https://doi.org/10.1016/j.ejpb.2016.05.020.

Peter, S., Lammens, R.F., Steffens, K.-J., 2010. Roller compaction/Dry granulation: Use of the thin layer model for predicting densities and forces during roller compaction. Powder Technol. 199 (2), 165–175. https://doi.org/10.1016/j.powtec.2010.01.002.

Reimer, H.L., Kleinebudde, P., 2019. Hybrid modeling of roll compaction processes with the Styl'One Evolution. Powder Technol. 341, 66–74. https://doi.org/10.1016/j.powtec.2018.02.052.

Roberts, R.J., Rowe, R.C., 1987. The compaction of pharmaceutical and other model materials - a pragmatic approach. Chem. Eng. Sci. 42 (4), 903–911. https://doi.org/10.1016/0009-2509(87)80048-9.

Rowe, J.M., Charlton, S.T., McCann, R.J., 2017. Chapter 32 - Development, Scale-Up, and Optimization of Process Parameters: Roller Compaction Theory and Practice. In: Qiu, Y. (Ed.), Developing Solid Oral Dosage Forms. Academic Press, Boston, pp. 869–915. https://doi.org/10.1016/B978-0-12-802447-8.00032-7.

Sakwanichol, J., Puttipipatkhachorn, S., Ingenerf, G., Kleinebudde, P., 2012. Roll compaction/dry granulation: Comparison between roll mill and oscillating granulator in dry granulation. Pharm. Dev. Technol. 17 (1), 30–39. https://doi.org/10.3109/10837450.2010.508078.

Souihi, N., Reynolds, G., Tajarobi, P., Wikström, H., Haeffler, G., Josefson, M., Trygg, J., 2015. Roll compaction process modeling: Transfer between equipment and impact of process parameters. Int. J. Pharm. 484 (1), 192–206. https://doi.org/10.1016/j.ijpharm.2015.02.042.

Sun, W.-J., Sun, C.C., 2017. Ribbon thickness influences fine generation during dry granulation. Int. J. Pharm. 529 (1), 87–88. https://doi.org/10.1016/j.ijpharm.2017.06.038.

Vasudevan, K.V., Pu, Y.E., Amini, H., Guarino, C., Agrawal, A., Akseli, I., 2022. Using a Model-based Material Sparing Approach for Formulation and Process Development of a Roller Compacted Drug Product. Pharm. Res. https://doi.org/10.1007/s11095-022-03192-3.

Wiedey, R., Kleinebudde, P., 2017. The Density Distribution in Ribbons from Roll Compaction. Chem. Ing. Tech. 89 (8), 1017–1024. https://doi.org/10.1002/cite.201600143.

Wu, S.-J., Sun, C., 2007. Insensitivity of compaction properties of brittle granules to size enlargement by roller compaction. J. Pharm. Sci. 96 (5), 1445–1450. https://doi.org/10.1002/jps.20929.

Zinchuk, A.V., Mullarney, M.P., Hancock, B.C., 2004. Simulation of roller compaction using a laboratory scale compaction simulator. Int. J. Pharm. 269 (2), 403–415. https://doi.org/10.1016/j.ijpharm.2003.09.034.